Exact time autocorrelation function of the *N*-spin classical Heisenberg equivalent neighbor model

Richard A. Klemm* and Marco Ameduri†
Max-Planck-Institut für Physik komplexer Systeme, Nöthnitzer Straße 38, D-01187 Dresden, Germany
(Received 10 April 2002; published 20 June 2002)

We reduce the autocorrelation function $\mathcal{C}_{11}(t)$ of the equivalent neighbor model of N classical spins exhibiting Heisenberg dynamics and exchange coupling J to quadrature. As the temperature $T\to\infty$, $\mathcal{C}_{11}(t)\propto t^{-N}$ for $Jt\gg 1$. At low T, the antiferromagnetic $\mathcal{C}_{11}(t)$ is a simple function of $(JT)^{1/2}t$, exhibiting strong frustration, but the ferromagnetic $\mathcal{C}_{11}(t)$ oscillates in a single mode, the frequency of which approaches NJ as $T\to 0$. We conjecture that as $T\to\infty$, the near-neighbor correlation functions of N-spin classical Heisenberg rings are simply obtained from these results.

DOI: 10.1103/PhysRevB.66.012403 PACS number(s): 75.10.Hk, 05.20.−y, 05.45.−a, 75.75.+a

Recently, there has been a considerable interest in the physics of magnetic molecules.[1] These consist of small clusters of magnetic ions imbedded within a nonmagnetic ligand group, which may crystallize into large, well-ordered single crystals of sufficient quality for neutron-scattering studies. Each molecule is characterized by the number N of spins and by their spatial configuration. Many examples of rings exist,[2,3] but there are also examples of denser clusters.[1,4] Usually, the spins interact mainly via the Heisenberg exchange interaction. Although interest in the dynamics of Heisenberg spin rings has been strong for many years, most of the work involved numerical simulation of the two-spin correlation functions. Recently, however, exact results for the Heisenberg dimer, isosceles and equilateral triangle, and four-spin ring were presented,[5–7] but larger rings cannot be solved using this technique.

The equivalent neighbor, or Kittel-Shore model, is the simplest model for the dynamics of a nanomagnet.[8] In this model, every spin interacts equally with all of the others. The Heisenberg dynamics were obtained previously in the $N\to\infty$ limit at infinite temperature T,[9] but have not been found for $5\leqslant N<\infty$. Although most molecules with $N\geqslant 5$ are more complicated,[1] there are few exactly solvable models of arbitrary N interacting spins with nonlinear dynamics in statistical mechanics. Hence its solution should be a benchmark for future theoretical and experimental studies.

In this paper, we present an exact single integral representation of the autocorrelation function $\mathcal{C}_{11}(t)$ for the equivalent neighbor model with arbitrary N and T, both for ferromagnetic (FM) and antiferromagnetic (AFM) exchange couplings. As $T\to\infty$, an accurate asymptotic $1/N$ expansion is found. As $T\to 0$, the AFM $\mathcal{C}_{11}(t)$ reduces to an exact scaling function of $(JT)^{1/2}t$ for arbitrary N. As $T\to 0$, the FM $\mathcal{C}_{11}(t)$ oscillates in a single mode with a frequency $\omega_N^*\to NJ$, and a shape that fits a new scaling form. From studies of three- and four-spin rings with additional bridging spins that interact only with the ring spins, we conjecture that as $T\to\infty$, the near-neighbor correlation functions $\mathcal{C}_{12}(t)$ in the N-spin equivalent neighbor and ring models are identical.

In the integrable Hamiltonian $H=-Js^2/2$ of the N-spin classical Heisenberg equivalent neighbor model,[10] the total spin $\mathbf{s}=\sum_{i=1}^{N}\mathbf{s}_i(t)$ is a constant. The dynamics are given by $d\mathbf{s}_i(t)/dt=J\mathbf{s}_i\times\mathbf{s}$, where $s_i=|\mathbf{s}_i|=1$. For $i=1$, $\mathbf{s}_1(t)=s_{1,||}\hat{\mathbf{s}}+s_{1,\perp}[\hat{\mathbf{x}}\cos(st^*)-\hat{\mathbf{y}}\sin(st^*)]$, where $t^*=Jt$, $\hat{\mathbf{s}}=\hat{\mathbf{x}}\times\hat{\mathbf{y}}$, $s_{1,||}=(s^2+1-x^2)/(2s)$, $x=|\mathbf{s}-\mathbf{s}_1|$, and $s_{1,||}^2+s_{1,\perp}^2=1$. Letting $\alpha=J/(2k_BT)$, where k_B is Boltzmann's constant, the autocorrelation function $\mathcal{C}_{11}(t)=\langle\mathbf{s}_1(t)\cdot\mathbf{s}_1(0)\rangle$ may be written

$$\mathcal{C}_{11}(t)=\frac{1}{Z_N}\int_0^{N-1}dx\mathcal{D}_{N-1}(x)\int_{|x-1|}^{x+1}se^{\alpha s^2}ds\times[s_{1,||}^2+\cos(st^*)s_{1,\perp}^2],\tag{1}$$

where the partition function $Z_N=\int_0^N 2s\mathcal{D}_N(s)e^{\alpha s^2}ds$ and $\mathcal{D}_N(x)$ is the N-spin density of states. To obtain $\mathcal{D}_N(x)$, we write Z_N in terms of integrals over $\mathbf{s}$, $\mathbf{s}-\mathbf{s}_1$, and each $\mathbf{s}_i$, with two constraints, written as integrals over $\mathbf{p},\mathbf{k}$.[6] Inverting the integration order, we obtain the integral representation, $\mathcal{D}_N(x)=\int_0^\infty 2p^{1-N}dp\,\sin^N p\sin px/\pi$. We expand $\sin^N p$ for N even [odd] in terms of $\cos(2mp)$ [$\sin(2m+1)p$],[11] and integrate by parts, using $\int_0^\infty\sin(px)dp/p=\pi\,\mathrm{sgn}(x)/2$. After rearranging, $\mathcal{D}_N(x)$ is piecewise continuous,

$$\mathcal{D}_N(x)=\Theta(x)\sum_{p=0}^{E[(N-1)/2]}\Theta(N-2p-x)\times\Theta(x-N+2p+2)d_{N-2p}(x),\tag{2}$$

$$d_{N-2p}(x)=\sum_{k=0}^{p}\frac{(-1)^k(N-2k-x)^{N-2}}{2^{N-1}(N-2)!}\binom{N}{k},\tag{3}$$

where $\Theta(x)$ is the Heaviside step function and $E(x)$ is the largest integer in x. Further details will be presented elsewhere.[12] $\mathcal{C}_{12}(t)=\langle\mathbf{s}_1(t)\cdot\mathbf{s}_2(0)\rangle$ is then found from the sum rule $\langle s^2\rangle/N=(N-1)\mathcal{C}_{12}(t)+\mathcal{C}_{11}(t)$.

It is useful to write $\delta\mathcal{C}_{11}(t)=\mathcal{C}_{11}(t)-\lim_{t\to\infty}\mathcal{C}_{11}(t)$. Since $\mathcal{C}_{11}(0)=1$, it suffices to obtain $\delta\mathcal{C}_{11}(t)$ for all t. We first invert the integration order in Eq. (1). The integration region is the interior of the irregular quadrangle formed by the lines $s=1-x$, $s=x\pm 1$, and $x=N-1$. We break this up into the interiors of the triangle formed by $x-1=\pm s$ and $s=1$, the parallelogram formed by $s=1$, $s=N-2$, and $x=s\pm 1$, and the triangle formed by $s=N-2$, $x=N-1$, and $x=s-1$. Making extensive use of symbolic manipulation software to integrate these regions with respect to x, we reduced $\delta\mathcal{C}_{11}(t)$

to a sum of single integrals, giving an exact expression for the piecewise continuous Fourier transform,[12]

$$\delta\mathcal{C}_{11}(t)=\sum_{p=0}^{E[(N-1)/2]}\int_{N-2p-2}^{N-2p}ds\,\cos(st^*)f_{N-2p}(s), \quad (4)$$

$$f_{N-2p}(s)=\Theta(s)\frac{e^{\alpha s^2}}{Z_N}\sum_{k=0}^{p}(N-2k-s)^{N-1}g_k(s), \quad (5)$$

$$g_0(s)=\frac{(N-1)a(s)}{2^{N-3}s(N+2)!}, \quad (6)$$

$$a(s)=N(s+1)^3-N^2(s+1)+N+s^3-2s, \quad (7)$$

$$g_k(s)=\frac{(-1)^k b_{N-2k}(s)}{s2^{N-3}N(N+2)!}\binom{N}{k}, \quad k\neq 0, \quad (8)$$

$$b_m(s)=s^2N(N-1)[3m+s(N+1)]+[s(N-1)+m]\times[6m^2-N(N+1)(N+2)]. \quad (9)$$

To obtain the long-time asymptotic behavior for $|\alpha|\ll 1$, we integrate Eq. (4) by parts $N-1$ times. We find

$$\delta\mathcal{C}_{11}(t)\underset{t^*\gg 1}{\sim}\sum_{p=0}^{E(N/2)}(t^*)^{-N}\cos[(N-2p)(t^*-\pi/2)]\times e^{(N-2p)^2\alpha}[1+(p-1)\delta_{p,N/2}]\times\frac{[(N-2p)^2-N]}{2^{N-3}NZ_N}\binom{N}{p}. \quad (10)$$

For $N=M^2$, one of the terms in Eq. (10) vanishes, as for the four-spin ring.[6] More important, the leading long-time behavior $\propto 1/t^{*N}$. Although Eq. (10) fails for $|\alpha|\gg 1$, its behavior for $\alpha\neq 0$ is useful to illuminate the dramatic difference between the long-time asymptotic behavior for the FM and AFM cases. For the FM case, $\alpha>0$, the dominant behavior $\propto\cos[N(t^*-\pi/2)]$, as the spins tend to oscillate together. In the AFM case, $\alpha<0$, the dominant long-time asymptotic behavior is given by the smallest possible oscillation frequency. As shown in the following, $\mathcal{C}_{11}(t)$ is always finite as $T\to 0$.

Liu and Müller solved for $\mathcal{C}_{11}$ as $N,T\to\infty$ by rescaling $J\to J'/\sqrt{N}$ and letting $N\to\infty, J\to 0$, keeping J' fixed.[9] This procedure is not extendable to finite N. In the integral representation for $\mathcal{D}_N(x)$, we expand $\sin^N p/p^N$ as $\exp[-N(p^2/6+p^4/180+p^6/2835+\cdots)]$ to obtain a $1/N$ asymptotic expansion for $\mathcal{C}_{11}(t)$ as $T\to\infty$,

$$\lim_{\substack{T\to\infty\\ N\gg 1}}\mathcal{C}_{11}(t)\sim[1+2e^{-\tilde{t}^2}(1-2\tilde{t}^2)]/3+2[1-e^{-\tilde{t}^2}(1+\tilde{t}^2-\tilde{t}^4/3-2\tilde{t}^6)]/(5N)+\frac{12}{175N^2}\left[1-e^{-\tilde{t}^2}\left(1+\tilde{t}^2-\frac{157}{36}\tilde{t}^4+\frac{50}{27}\tilde{t}^6-\frac{97}{108}\tilde{t}^8+\frac{7}{18}\tilde{t}^{10}\right)\right], \quad (11)$$

where $\tilde{t}=Jt[(N-1)/6]^{1/2}$. From Eq. (11), $\mathcal{C}_{11}(0)=1$ through order $1/N^2$, as required, and $\mathcal{C}_{11}(t)$ has the correct $N\to\infty$ limit.[9] However, Eq. (11) is highly accurate for intermediate N values as well. In Fig. 1, we have plotted $\lim_{T\to\infty}\mathcal{C}_{11}(t)$ for $N=5,6,7,8,9,25,50,100,\infty$ as a function of $Jt[(N-1)/6]^{1/2}$. The curves for $N=25,50,100,\infty$ were obtained from Eq. (11), whereas the other curves were generated from the exact solution, Eqs. (4)–(9). Equation (11) is very accurate at short and long times, even for $N=5$. We note that for $\tilde{t}\lesssim 1$, $\lim_{T\to\infty}\mathcal{C}_{11}(t)$ is a universal function of $Jt\sqrt{N-1}$, as suggested by the $1/N$ expansion. Although the $N\to\infty$ curve is exact, and the curves for $N=50,100$ are quite accurate, the curve for $N=25$ exhibits a small ($\approx 1\%$) inaccuracy for $1.2\lesssim\tilde{t}\lesssim 2.2$.

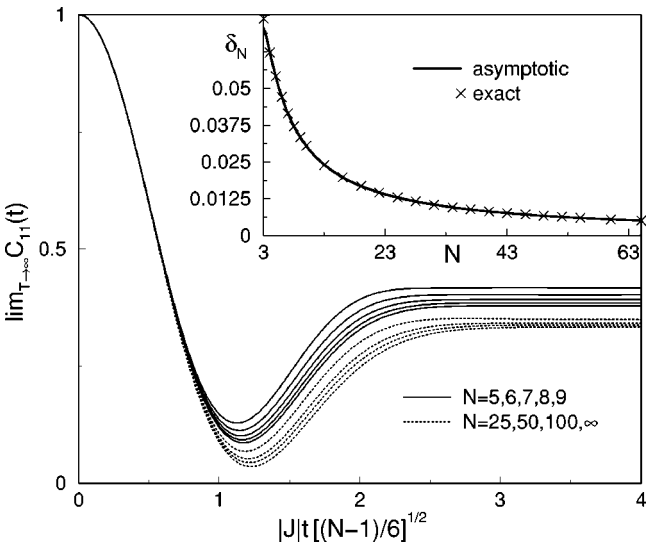

FIG. 1. Plots of $\lim_{T\to\infty}\mathcal{C}_{11}(t)$ versus $|J|t[(N-1)/6]^{1/2}$, for $N=5,6,7,8,9$ from Eqs. (4)–(9) (solid), and for $N=25,50,100,\infty$ from Eq. (11) (dashed). Inset: Plot of the exact ($\times$) and asymptotic values, Eq. (13), of δ_N.

At arbitrary N,t and $N\gg 1, t\to\infty$, respectively,

$$\lim_{T\to\infty}\mathcal{C}_{11}(t)=1/N+(N-1)[\delta_N+f_N(t)], \quad (12)$$

$$\delta_N\underset{N\gg 1}{\sim}\frac{175N^2-315N+36}{525N^2(N-1)}, \quad (13)$$

where the asymptotic Eq. (13) is obtained from Eq. (12) and $\lim_{t,T\to\infty}\mathcal{C}_{11}\sim\frac{1}{3}+2/5N+12/175N^2$ for $N\gg 1$. In the inset of Fig. 1, we compare the exact values of δ_N with those obtained from Eq. (13) for $3\leq N\leq 65$. As N increases from 5 to 65, the relative difference decreases rapidly from 0.14% to 0.2 ppm. Since the exact formula for δ_N with N odd (even) contains nontrivial contributions of logarithms of all prime numbers from 3 to N (2 to $N/2$), respectively, this extremely good numerical agreement is remarkable.

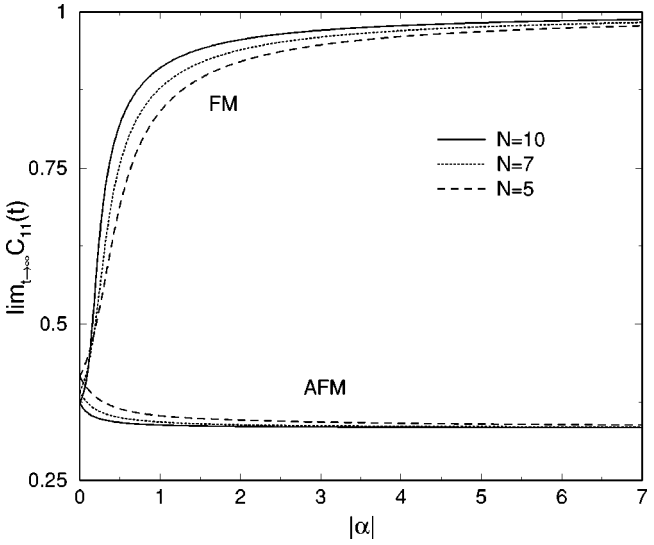

FIG. 2. Plots of $\lim_{t\to\infty}\mathcal{C}_{11}(t)$ versus $|\alpha|$ for $N=5,7,10$ and for both ferromagnetic and antiferromagnetic couplings.

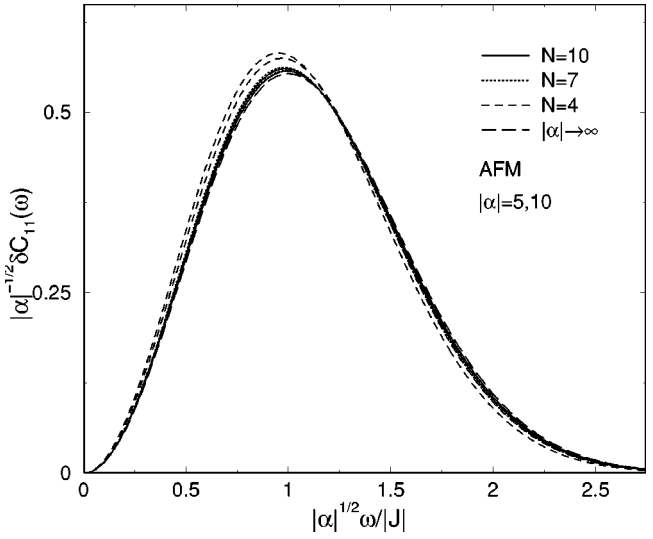

FIG. 3. Plots of the low-T $|\alpha|^{-1/2}\delta\mathcal{C}_{11}(\omega)$ versus $|\alpha|^{1/2}\omega/|J|$ for the antiferromagnetic cases with $N=4,7,10$ at $\alpha=-5,-10$. Also shown is the exact $T\to 0$ limit, Eq. (14).

In Fig. 2, we plot $\lim_{t\to\infty}\mathcal{C}_{11}(t)$ for both the FM and AFM cases, for $N=5,7,10$, as functions of $|\alpha|$. The FM values approach 1 as $T\to 0$, but the low-T AFM values rapidly approach their $T=0$ limit, $\frac{1}{3}$. This indicates that the spins are strongly frustrated, since one might expect the AFM $\lim_{t\to\infty}\mathcal{C}_{11}(t)=0$, as for the four-spin ring.[6] In that case, the unfrustrated alternating spin configuration was possible. In this AFM case, however, as $T\to 0$ the $N\geqslant 3$ spins are as frustrated as are an infinite number of them as $T\to\infty$.

For the low-T AFM dynamics, the dominant contributions to the numerator of $\mathcal{C}_{11}$ and to Z_N arise from $s\ll 1$. They have the forms $P_N s^2 e^{-|\alpha|s^2}$ and $Q_N s^2 e^{-|\alpha|s^2}$, respectively, where P_N and Q_N are complicated functions of N, but for arbitrary $N\geqslant 3, P_N/Q_N=\frac{2}{3}$. Thus, as $T\to 0$, the Fourier transform $\delta\mathcal{C}_{11}(\omega)$ of $\delta\mathcal{C}_{11}(t)$ attains the exact uniform asymptotic scaling form,

$$|\alpha|^{-1/2}\delta\mathcal{C}_{11}(\omega)\underset{T\to 0}{\sim}\frac{8}{3\sqrt{\pi}}\tilde{\omega}^2 e^{-\tilde{\omega}^2}, \tag{14}$$

where $\tilde{\omega}=|\alpha|^{-1/2}\omega/|J|$. For $N\geqslant 5$, corrections to Eq. (14) are of $\mathcal{O}(|\alpha|^{-1})$, whereas for $N=4$, they are of $\mathcal{O}(|\alpha|^{-1/2})$. In Fig. 3, we plot $|\alpha|^{-1/2}\delta\mathcal{C}_{11}(\omega)$ vs $|\alpha|^{1/2}\omega/|J|$ of the low-T AFM mode at $\alpha=-5,-10$ for $N=4,7,10$, from our exact solution, Eqs. (4)–(9). The exact asymptotic form, Eq. (14), is also plotted for comparison. The $N=4$ curves nearly coincide with the others, but do show some small dependence upon T. However, the $N=7$ and 10 curves are nearly identical and independent of T, and are nearly indistinguishable from the asymptotic curve for $|\alpha|=10$.

Inverting the Fourier transform, the low-T AFM $\mathcal{C}_{11}(t)$ asymptotically approaches

$$\mathcal{C}_{11}(t)\underset{T\to 0}{\sim}[1+2e^{-\bar{t}^2}(1-2\bar{t}^2)]/3, \tag{15}$$

where $\bar{t}=t^*/(2|\alpha|^{1/2})$. Hence the AFM $\lim_{T\to 0}\mathcal{C}_{11}(t)$ is a uniform function of $(JT)^{1/2}t$, independent of N. Moreover, it has precisely the same form as does $\lim_{N,T\to\infty}\mathcal{C}_{11}(t)$, Eq. (11), pictured in Fig. 1, except for the different scaling factor.

We now turn to the FM case as $T\to 0$. From Eq. (10), we expect all of the spins to oscillate together with frequency NJ at $T=0$. At finite T, the oscillation frequency deviates from this value slightly. To determine the precise nature of the mode, we note that for $\alpha>1$, the peaks in the integrand and in Z_N both occur within $N-2\leqslant s\leqslant N$. As $T\to 0$, we evaluate Z_N by integration by parts, leading to the exact low-T limit,

$$\delta\mathcal{C}_{11}(\omega)\underset{T\to 0}{\sim}A_N f_N(\omega^*)/f_N(\omega_N^*), \tag{16}$$

where $A_N=2e[(N-1)/e]^N/N!$, $\omega^*=\omega/J$, and ω_N^*, the position of the exact maximum in $f_N(\omega^*)$, is an eigenvalue of $2\alpha s-(N-2)/(N-s)+d\ln[g_0(s)]/ds=0$. f_N and g_0 are given by Eqs. (5) and (6), respectively. Then $\omega_N^*\approx N-(N-1)/(2N\alpha)$, and $f_N(\omega^*)$ has a width characterized by a normal Gaussian distribution parameter $\sigma_N=\sqrt{N-1}/(2N\alpha)$. Thus

$$\delta\mathcal{C}_{11}(\omega)\underset{\alpha\gg 1}{\approx}A_N\exp[-(\omega^*-\omega_N^*)^2/(2\sigma_N^2)]. \tag{17}$$

In this approximation, ω_N^*, σ_N, and A_N are correctly given to their respective leading orders in $1/\alpha$, but the skewness of the peak is not accurately represented. Thus in Fig. 4 we plotted the low-T $\delta\mathcal{C}_{11}(\omega)/A_N$ versus $(\omega^*-\omega_N^*)N\alpha/\sqrt{N-1}$, for $N=8$ at $\alpha=5,10$, and for $N=5$ at $\alpha=5,10,28$, using our exact formulas, Eqs. (4)–(9). The $N=5$ curves nearly coincide, as do the $N=8$ curves, and the scaled height approaches 1 as $T\to 0$. The asymmetry of the curves decreases with increasing N. Nevertheless this new

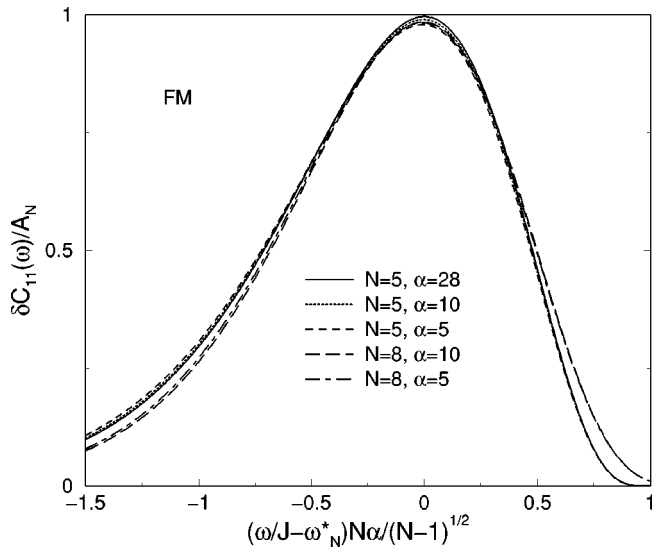

FIG. 4. Plots of the low-T $\delta\mathcal{C}_{11}(\omega)/A_N$ versus $(\omega/J-\omega_N^*)N\alpha/\sqrt{N-1}$, where $\omega_N^*=N-(N-1)/(2N\alpha)$ and $A_N=2e[(N-1)/e]^N/N!$, for the FM cases with $N=8,\alpha=5,10$, and $N=5,\alpha=5,10,28$.

scaling procedure works remarkably well, and $N=5$ is close to the large N limit, even for the FM case.

Inverting the low-T FM Fourier transform, Eq. (17),

$$\mathcal{C}_{11}(t) \underset{T\to 0}{\approx} 1-\frac{B_N}{\alpha}[1-e^{-t^{*2}\sigma_N^2/2}\cos(\omega_N^* t^*)], \qquad (18)$$

where $B_N=A_N\sqrt{\pi(N-1)/2}/N$. As $N\to\infty$, $B_N\to 1/N$. The deviation of the long-time limit of Eq. (18) agrees to within 1% with our results presented in Fig. 2. The decay in time of the mode in this approximation is Gaussian, with a lifetime $\tau_N=1/\sigma_N$. Thus, as $T\to 0$, the oscillations are characterized by a frequency that approaches NJ linearly in T, a lifetime that diverges as $1/T$, and an amplitude that vanishes as T.

Finally, we conjecture that, as for the N-spin equivalent neighbor model,

$$\lim_{T\to\infty}\mathcal{C}_{12}(t)=1/N-\delta_N-f_N(t) \qquad (19)$$

for the classical N-spin ring with near-neighbor coupling. We first note that Eq. (19) is valid for four- and three-spin rings.[6,7] In further support of this conjecture, we have studied the N-spin systems consisting of M spins $\mathbf{s}_j'$ coupled to $N-M$ spins $\mathbf{s}_i$ on a ring. Letting $\mathbf{s}=\Sigma_{i=1}^{N-M}\mathbf{s}_i$ and $\mathbf{s}'=\Sigma_{j=1}^{M}\mathbf{s}_j'$, the integrable Hamiltonian is $-J\Sigma_{i=1}^{N-M}\mathbf{s}_i\cdot\mathbf{s}_{i+1}-J'\mathbf{s}\cdot\mathbf{s}'$, where $\mathbf{s}_{N-M+1}=\mathbf{s}_1$.[10] For $(M,N)=(2,6)$, the square diamond or four-spin ring with $\mathbf{s}=\mathbf{s}_{13}+\mathbf{s}_{24}$ and two apical spins with $\mathbf{s}'=\mathbf{s}_1'+\mathbf{s}_2'$, we let $\mathbf{S}=\mathbf{s}+\mathbf{s}'$. At $T\to\infty$, the integrals over s_{13} and s_{24} can be combined. Setting $\mathcal{C}'(t)=\langle\mathbf{s}'(t)\cdot\mathbf{s}'(0)\rangle$, we found

$$\lim_{T\to\infty}\mathcal{C}'(t)=\frac{1}{Z}\int_0^2 ds'\int_0^4\mathcal{D}_4(s)ds\int_{|s-s'|}^{s+s'}SdS \times[s_\parallel'^2+\cos(St')s_\perp'^2], \qquad (20)$$

where $t'=J't$, $s_{||}'=(S^2-s^2+s'^2)/(2S)$ and $s_\perp'^2+s_\parallel'^2=s'^2$, and Z at $T\to\infty$ is given by the first line of Eq. (20). Performing the integrals exactly, we find

$$\lim_{T\to\infty}\mathcal{C}'(t)=\frac{2}{3}+8[\delta_6+f_6(t')], \qquad (21)$$

where δ_6 and $f_6(t)$ are precisely the same as for the $N=6$ equivalent neighbor model as $T\to\infty$ in Eq. (12). Altogether, we found for $N-M=3$, $M=1,2,3$, and for $N-M=4$, $M=1,2$, that

$$\lim_{T\to\infty}\mathcal{C}'(t)=M^2/N+M(N-M)[\delta_N+f_N(t')]. \qquad (22)$$

In summary, we have solved exactly for the time autocorrelation function $\mathcal{C}_{11}(t)$ of a spin in the N-spin equivalent neighbor model. As $T\to\infty$, $\mathcal{C}_{11}(t)\propto t^{-N}$ for $Jt\gg 1$, curves for different N exhibit very similar shapes when plotted as functions of $|J|t[(N-1)]^{1/2}$, and an accurate $1/N$ asymptotic expansion is found. At low T, the antiferromagnetic $\mathcal{C}_{11}(t)$ fits an exact, universal scaling function of $tT^{1/2}$, independent of N, and exhibits strong frustration. For the ferromagnetic case at low T, there is a single mode with a peak position at $\approx NJ-k_BT(N-1)/N$, and a shape that fits an accurate, new scaling relation. We conjecture that the $T\to\infty$ limit of the near-neighbor correlation functions $\mathcal{C}_{12}(t)$ for the N-spin equivalent neighbor model and for the N-spin ring may be identical.

*Electronic address: rklemm@mpipks-dresden.mpg.de
†Electronic address: marco@mpipks-dresden.mpg.de

[1] D. Gatteschi, A. Caneschi, L. Pardi, and R. Sessoli, Science **265**, 1054 (1994).
[2] A. Lascialfari, D. Gatteschi, F. Borsa, and A. Cornia, Phys. Rev. B **55**, 14 341 (1997).
[3] M. H. Julien, Z. H. Jang, A. Lascialfari, F. Borsa, M. Horvatic, A. Caneschi, and D. Gatteschi, Phys. Rev. Lett. **83**, 227 (1999).
[4] R. Caciuffo, G. Amoretti, A. Murani, R. Sessoli, A. Caneschi, and D. Gatteschi, Phys. Rev. Lett. **81**, 4744 (1998).
[5] M. Luban and J. Luscombe, Am. J. Phys. **67**, 1161 (1999).
[6] R. Klemm and M. Luban, Phys. Rev. B **64**, 104424 (2001); cond-mat/0105050 (unpublished).
[7] M. Ameduri and R. Klemm, cond-mat/0108213 (unpublished).
[8] C. Kittel and H. Shore, Phys. Rev. **138**, A1165 (1965).
[9] J.-M. Liu and G. Müller, J. Appl. Phys. **67**, 5489 (1990); Phys. Rev. A **42**, 5854 (1990).
[10] N. Srivastava, C. Kaufman, G. Mueller, R. Weber, and H. Thomas, Z. Phys. B: Condens. Matter **70**, 251 (1988).
[11] I. S. Gradsteyn and I. M. Ryzhik, *Tables of Integrals, Series, and Products* (Academic, New York, 1965).
[12] R. A. Klemm and M. Ameduri (unpublished).